



HAL
open science

Crustal differentiation in the early solar system: clues from the unique achondrite Northwest Africa 7325 (NWA 7325)

Jean-Alix J-A Barrat, R. C. Greenwood, A. Verchovsky, Ph Gillet, C Bollinger, Jessica Langlade, Céline C. Liorzou, I.A. Franchi

► To cite this version:

Jean-Alix J-A Barrat, R. C. Greenwood, A. Verchovsky, Ph Gillet, C Bollinger, et al.. Crustal differentiation in the early solar system: clues from the unique achondrite Northwest Africa 7325 (NWA 7325). *Geochimica et Cosmochimica Acta*, 2015, in press. insu-01178091

HAL Id: insu-01178091

<https://insu.hal.science/insu-01178091>

Submitted on 17 Jul 2015

HAL is a multi-disciplinary open access archive for the deposit and dissemination of scientific research documents, whether they are published or not. The documents may come from teaching and research institutions in France or abroad, or from public or private research centers.

L'archive ouverte pluridisciplinaire **HAL**, est destinée au dépôt et à la diffusion de documents scientifiques de niveau recherche, publiés ou non, émanant des établissements d'enseignement et de recherche français ou étrangers, des laboratoires publics ou privés.

26

Abstract

27 The unique achondrite NWA 7325 is an unusual olivine gabbro composed chiefly of calcic
28 plagioclase (An_{85-93}), diopsidic pyroxene ($En_{50.1-54.0} Wo_{44.8-49.3} Fs_{0.6-1.3}$), and forsteritic olivine (Fo_{97}). It
29 is Al and Mg-rich and Fe and Na-poor and displays very low concentrations of incompatible trace
30 elements, much below 0.3 x CI abundances for many of them. It is also characterized by huge Eu and
31 Sr anomalies ($Eu/Eu^*=65$, $Sr_n/Ce_n=240$). Although the O isotopic composition of NWA 7325 and
32 some ureilites (those with olivine cores in the range Fo_{75} to Fo_{88}) are similar, a genetic relationship
33 between them is unlikely due to the Fe-poor composition of NWA 7325. It is almost certainly derived
34 from a distinct planetesimal, not previously sampled by other achondrites. The low Na/Al, Ga/Al,
35 Zn/Al ratios as well as the low K, Rb and Cs shown by NWA 7325, suggest a volatile-depleted parent
36 body. This unique gabbro is demonstrably a cumulate, but the composition of its parental melt cannot
37 be precisely assessed. However, the liquid from which NWA 7325 crystallized would have been very
38 poor in incompatible trace elements (Yb in the range of 0.25 to 1.5 x CI abundance) with a very large
39 positive Eu anomaly. Such a melt cannot be the product of the early magmatic activity on a small
40 parent body. Instead, we propose that the parental melt to NWA 7325 formed as a consequence of the
41 total melting of an ancient gabbroic lithology, possibly upon impact, in agreement with the systematics
42 of ^{26}Al - ^{26}Mg . Based on recent dating, the crustal material that was parental to NWA 7325 must have
43 been older than 4562.8 Ma, and formed possibly ≈ 4566 Ma ago. If this scenario is correct, NWA 7325
44 provides evidence of one of the earliest crusts on a differentiated body so far studied.

45

46

47

48

49

50 **1. Introduction**

51 Achondrites are relatively rare extraterrestrial samples, which comprise only about 4 % of all
52 the recovered meteorites (Meteoritical Bulletin database). Most of them originated from small
53 differentiated bodies, while others were ejected from Mars, or the Moon, and so complement the
54 sampling undertaken during the Apollo and Luna programs. As a result, achondrites have a high
55 scientific value and, therefore, potentially can provide a unique insight into the processes that operated
56 on a variety of differentiated bodies in the early solar system.

57 The number of parent bodies sampled by achondrites is the subject of ongoing debate. About
58 95 % of these meteorites originated from only two bodies: 4-Vesta (the howardites, eucrites and
59 diogenites, ca. 1500 meteorites, 75 % of all achondrites) and the now-disrupted ureilite parent body
60 (ca. 400 meteorites, 20 % of all achondrites). Mars, the Moon and a handful of smaller bodies are the
61 sources of the remaining achondrites. Some of them form distinct groups based on their petrographic
62 and isotopic features, such as the aubrites, the angrites or the brachinites (see recent reviews by Keil,
63 2010, 2012, 2014). Others, as exemplified by Northwest Africa 011 (NWA 011, Yamaguchi et al.,
64 2002), are ungrouped and consequently unique samples of unidentified differentiated bodies. While it
65 is more likely that these unique achondrites originated from one of the many planetesimals that
66 differentiated during the first few million years of solar system history, the possibility that we have in
67 our collections an achondrite from Mercury (e.g., Love and Keil, 1995) cannot be wholly discounted.
68 Such a rock would not only provide essential constraints for models of the differentiation of this
69 planet, but for the chemical structure of the inner solar system too.

70 The recent discovery of Northwest Africa 7325 (NWA 7325) and its pairing (NWA 8014 and
71 8486) was stimulating. Thirty seven fragments totaling ca. 600 g, of an unusual achondrite displaying
72 a distinctive green fusion crust (Fig. 1a), were collected near Bir el Abbas, Morocco. Irving et al.
73 (2013) were the first to study this meteorite and to show that it consists of a unique gabbroic lithology.
74 They compared its major element composition to that of Mercury's surface, as determined by the
75 MESSENGER spacecraft (Weider et al., 2012), and suggested that this meteorite could have

76 originated from this planet. Subsequently, this rock has been extensively studied by different teams
77 using a variety of techniques (Irving et al., 2013; Amelin et al., 2013; Bischoff et al., 2013; Sanborn et
78 al., 2013; Dunlap et al., 2014; El Goresy et al., 2014; Goodrich et al., 2014; Jabeen et al., 2014; Kita et
79 al., 2014; Sutton et al., 2014; Weber et al., 2014, 2015; Archer et al., 2015). Although a mercurian
80 origin is not currently favored by most of these studies, this rock remains fascinating and scientifically
81 important by virtue of its distinct petrographic and geochemical features. Here we report new
82 chemical, mineralogical and stable isotope (oxygen, carbon and nitrogen) results that provide
83 important evidence relevant to the origin of this unique meteorite.

84

85 **2. Samples and analytical techniques**

86 Two samples of NWA 7325 were available for bulk rock chemical analysis: a clean chip of the
87 interior of the meteorite (600 mg, fragment of the same slice used for the thick section), and a sample
88 of cutting dust recovered using distilled water during cutting of the stones by S. Ralew, the owner of
89 the meteorite. In addition, two low-Ti gabbroic pebbles from Vaca Muerta were selected for
90 comparison, from the mesosiderite samples studied previously by Greenwood et al. (2006).
91 Petrographic observations and quantitative chemical analyses of the main phases of the NWA 7325
92 achondrite were made on a polished thick section (1 cm²) prepared from a slice obtained from S.
93 Ralew. Cameca SX100 electron microprobe analyses at Service Commun “Microsonde Ouest”
94 (Plouzané) were obtained at 15 kV accelerating voltage with a probe current of 12 nA. Minerals
95 [wollastonite (Si, Ca), orthoclase (K), albite (Na), apatite (P)], oxide [MnTiO₃ (Mn, Ti)], Al₂O₃ (Al),
96 Fe₂O₃ (Fe), Cr₂O₃ (Cr)], and one sulfide [FeS₂ (S)] were used for calibration. The raw data were
97 corrected with the ‘PAP’ software (Pouchou and Pichoir, 1985).

98

99 The Vaca Muerta samples and the NWA 7325 chip were totally powdered using a boron
100 carbide pestle and mortar. Major and trace element concentrations were determined respectively by
101 ICP-AES (inductively coupled plasma-atomic emission spectrometry) and ICP-MS (inductively

102 coupled plasma-mass spectrometry) at Université de Brest (IUEM, Plouzané) using the procedures
103 described by Barrat et al. (2012, 2014). The accuracy of major and trace element concentrations is
104 better than 5% (probably better than 3% for all the REEs) based on various standard and sample
105 duplicates.

106 Oxygen isotope analyses were carried out at the Open University using an infrared laser
107 fluorination system following the methods and procedures of Miller et al. (1999). Analyses were
108 undertaken using a powder prepared from the 600 mg internal sample of NWA 7325. Oxygen was
109 released from 2 mg aliquots by heating in the presence of BrF₅. After fluorination, the released oxygen
110 gas was purified by passing it through two cryogenic nitrogen traps and over a bed of heated KBr.
111 Oxygen gas was analysed using a MAT 253 dual inlet mass spectrometer. Interference at m/z=33 by
112 the NF₃ fragment ion NF⁺ was monitored by performing scans for NF₂⁺ on all samples run in this
113 study. In all cases NF₂ was either negligible or absent. Oxygen isotopic analyses are reported in
114 standard δ notation, where δ¹⁸O has been calculated relative to VSMOW (Vienna Standard Mean
115 Ocean Water) as δ¹⁸O = [(¹⁸O /¹⁶O_{sample}) / (¹⁸O /¹⁶O_{VSMOW}) - 1] x 1000 (‰) and similarly for δ¹⁷O using
116 the ¹⁷O /¹⁶O ratio. Δ¹⁷O, which represents the deviation from the terrestrial fractionation line, has been
117 calculated using a linearized format (Miller, 2002):

$$118 \quad \Delta^{17}\text{O} = 1000 \ln(1 + \delta^{17}\text{O}/1000) - \lambda 1000 \ln(1 + \delta^{18}\text{O}/1000)$$

119 where λ = 0.5247, which was determined using 47 terrestrial whole-rock and mineral separate samples
120 (Miller et al., 1999; Miller, 2002). Recent levels of precision obtained on the Open University system,
121 as demonstrated by 39 analyses of our internal obsidian standard, were as follows: ±0.05‰ for δ¹⁷O;
122 ±0.09‰ for δ¹⁸O; ±0.02‰ for Δ¹⁷O (2σ).

123 Carbon and nitrogen concentrations and isotopic analyses were obtained by the stepped
124 combustion technique using the multi-element analyzer system “Finesse” (Verchovsky et al., 1998,
125 2003). An aliquot (6.134 mg) of the internal sample of NWA 7325 was heated from 200 to 1400°C
126 with 100° increments. The released N and C in the form of N₂ and CO₂ were analyzed simultaneously

127 from the same aliquot. The isotope results are expressed in standard δ notation normalized to air for N
128 and to PDB for C.

129

130 **3. Results and discussion**

131 **3.1. Petrography**

132 NWA 7325 has been extensively described in a series of abstracts (Irving et al., 2013; Bischoff
133 et al., 2013; Goodrich et al., 2014; El Goresy et al., 2014). Our observations are in agreement with
134 these earlier studies, and are summarized here. NWA 7325 is a fine to medium grained gabbroic rock
135 with a grain size typically in the range of 0.5-1 mm (Fig. 1). It is unbrecciated, and consists of ~25-30
136 vol% diopsidic pyroxenes, ~15 vol% olivine grains surrounded or poikilitically enclosed by
137 plagioclase (~55-60 vol%), with accessory iron sulfides (1 vol%), and sparse ferrochromite, metal
138 grains and rare eskolaite associated with iron sulfide. El Goresy et al. (2014) report the occurrence of
139 Ca sulfates that they interpret as totally weathered grains of oldhamite. However, like the vast
140 majority of Saharan finds, NWA 7325 contains cracks filled with secondary carbonates. Rather than
141 being formed by the terrestrial alteration of oldhamite, we believe that the Ca sulfates in NWA 7325
142 are more likely to represent normal hot desert weathering products.

143 Major element compositions of the main phases are reported in Table 1. Coarse-grained
144 plagioclase is calcic (An_{85-93}), and contains traces of MgO (=0.13-0.45 wt%). Ca-pyroxene is
145 homogeneous and extremely magnesian ($En_{50.1-54.0}$ $Wo_{44.8-49.3}$ $Fs_{0.6-1.3}$, $Mg/(Fe+Mg)= 0.975-0.983$,
146 $n=58$). Olivine ($Fo_{97.97.3}$, $n=51$) is in equilibrium with pyroxene (e.g., Perkins and Vielzeuf, 1992). Fe-
147 sulfide is Cr-rich ($Cr = 2.2-6$ wt%) and contains lamellas of daubréelite.

148 Irving et al. (2013) noted that the plagioclase in NWA 7325 is finely mottled, and much less
149 birefringent than normal. It contains clusters of tiny grains of troilite and metal. They suggested that
150 the plagioclase has been totally melted, possibly as a result of shock, and reacted locally with olivine
151 to generate secondary diopside. This view has been challenged by Bischoff et al. (2013). They

152 observed plagioclase-rich veins and occasionally SiO₂-normative mesostases around mafic minerals
153 and within Ca-pyroxenes, which could have been formed upon shock. However, they pointed out that
154 olivine is only very weakly shocked (stage S2), suggesting that the shock pressure suffered by NWA
155 7325 was certainly not strong enough to melt it extensively.

156

157 3.2. Geochemistry

158 3.2.1. Major and trace element.

159 The major element composition of the cutting dust (Table 2) is very similar to the results
160 obtained at University of Alberta on a distinct sample of cutting dust (Irving et al., 2013). NWA 7325
161 is a basic rock, rich in MgO and Al₂O₃, and poor in Fe, Mn and alkalis (Na₂O = 0.6 wt%). Using the
162 average compositions of the main phases, it corresponds to an assemblage of about 55 wt%
163 plagioclase, 32 wt% pyroxene, 10 wt% olivine and traces of sulfides and secondary calcite, in
164 agreement with phase proportions estimated from the polished sections (see above).

165 Despite the similarity of their major element compositions, the trace element abundances of
166 the two cutting dust samples (this study and Irving et al., 2013) are different, and display some
167 significant discrepancies (Table 3 and Fig. 2 and 3). Both samples are poor in incompatible lithophile
168 elements (REEs except Eu < 2 x CI), light REE enriched (La_n/Sm_n = 1.95 – 2.90) with striking positive
169 Eu anomalies (Eu/Eu* = 16.1 – 35.2), but our sample contains respectively about 2x more light REEs,
170 and half the Th content reported by Irving et al. (2013). Furthermore, the Irving et al. (2013) sample
171 displays markedly high Nb and Hf abundances compared to our analysis. A number of possible
172 explanations might account for these differences: i) contamination during the cutting of the meteorite
173 by handling and by the saw blade, ii) different proportions of soil materials which were adhering to the
174 surface of the stones (see Fig. 1a), and, iii) different contributions from secondary phases (Fe-oxides,
175 carbonates and sulfates) along surfaces crossed by the saw blade. The low abundance of incompatible
176 lithophile elements (e.g., the light REEs, Th, U, Rb and Cs) makes them extremely sensitive to

177 terrestrial contamination, which could have taken place subsequent to its landing on the desert soil,
178 and/or by handling during the recovery and sample preparation. The soil of the strewnfield has not
179 been analyzed, but its Th and REE abundances are probably similar to those of the upper continental
180 crust average. Such a soil [as illustrated by the soil of Tatahouine (Barrat et al., 1999)] can contain ca.
181 100 times more La and Th than the cutting dust. A slight contamination by soil could be undetectable
182 with major elements, but have a huge impact on the abundances of many trace elements.

183 It is clear from the preceding section that the trace element composition of NWA 7325 should
184 be determined using material from clean interior chips. We prepared one such fraction using a
185 fragment weighing 600 mg. Its major element abundances deviate just slightly from the cutting dust
186 analyses, except for Fe which is three time less abundant in the chip than in the cutting dust.
187 Furthermore, the cutting dust contains much more Ni, Cu, Zn W and Pb than the interior chips, which
188 most likely result from contamination by the saw blade. We don't know exactly the composition of the
189 saw blade which was used here, but saw blades typically have diamond grit in them that are
190 electroplated to the steel blade with a Ni, Cu or Zn matrix. Therefore, most major element abundances
191 determined using cutting dust would appear to be representative of the whole rock, contrary to the
192 trace element contents which are not reliable and should be rejected (Tables 2 and 3).

193 Despite our effort to select a fragment that was as fresh as possible, terrestrial weathering
194 effects cannot be totally avoided. The mineralogical and chemical effects of hot desert weathering are
195 now relatively well understood, and have been previously documented in a range of meteorite types
196 (e.g., Barrat et al., 1999; 2004, 2010; Stelzner et al., 1999; Crozaz et al., 2003). Our interior chip is no
197 exception. As shown in Figures 2 and 3, it displays a high Ba abundance, a high U/Th ratio (= 1.1),
198 and a positive Ce anomaly ($Ce/Ce^* = 1.25$). Such features have been repeatedly observed in weathered
199 Saharan finds, and it is not necessary to repeat here a discussion concerning their origin. Although
200 Saharan finds display often high Sr abundances, the positive Sr anomaly exhibited by NWA 7325 is
201 probably, like the Eu anomaly, a primary feature attributable to plagioclase.

202

203 NWA 7325 contains low but significant amounts of Ni (= 57 $\mu\text{g/g}$) and Co (=23 $\mu\text{g/g}$),
204 probably hosted by minute grains of metal (Table 3). It is poor in Zn, Cu and Pb. Its low lithophile
205 element abundances are well illustrated by the CI- normalized trace element patterns (Fig. 2 and 3).
206 Except for Sc, Ba, U, Sr and Eu, all the lithophile trace elements display concentration $< 0.3 \times \text{CI}$.
207 Furthermore, the trace element patterns exhibit Cs, Rb, Zr, and Hf depletions. Contrary to the results
208 for the cutting dust, the interior fragment is light-REE depleted ($\text{La}_n/\text{Sm}_n = 0.70$), and displays large
209 positive Eu and Sr anomalies ($\text{Eu}/\text{Eu}^* = 65$, $\text{Sr}_n/\text{Ce}_n = 240$).

210

211 3.2.2. Oxygen isotopes.

212 The bulk oxygen isotopic composition of NWA 7325 was determined in duplicate using the powder
213 made with the interior fragment. The average of the two analyses was: $\delta^{17}\text{O} = 3.33 \pm 0.09 \text{‰}$, $\delta^{18}\text{O} =$
214 $8.10 \pm 0.18 \text{‰}$, $\Delta^{17}\text{O} = -0.91 \pm 0.01 \text{‰}$ (errors $\pm 1\sigma$). Our new analysis of NWA 7325 plots on the
215 CCAM line in Fig. 4, within the ureilite field. Three individual analyses of NWA 7325 by Irving et al.
216 (2013) have somewhat divergent compositions, with one plotting close to the result reported here.
217 Jabeen et al. (2014) give oxygen isotope analyses for plagioclase and pyroxene mineral separates from
218 NWA 7325 that are displaced from one another by approximately 2 ‰ along a mass fractionation line
219 (Fig. 4). The mean plagioclase analysis (n=4) of Jabeen et al. (2014) plots close to our bulk value for
220 NWA 7325. However, in view of the significant proportion of pyroxene in NWA 7325 (20-30 %, section 3.1) the analyses of Jabeen suggest that, had they determined a bulk composition for the
221 meteorite, this would probably have been shifted to somewhat lower $\delta^{18}\text{O}$ values compared to our
222 analysis.
223

224

225 3.2.3. Carbon and nitrogen isotopes.

226 The results for C and N are presented in table 4 and Figure. 5. Carbon displays a bimodal
227 release with peaks in the range 200-400°C and 500-700°C. The low temperature peak is due to the

228 terrestrial contamination associated with both weathering during the residence of the meteorite on the
229 Earth's surface and laboratory handling and has a characteristic carbon isotopic composition ($\delta^{13}\text{C} = -$
230 27 to -29%). The second peak seems to represent a terrestrial carbonate as indicated both by the
231 release temperature corresponding to that for decomposition of CaCO_3 and the isotopic composition
232 with $\delta^{13}\text{C} = -1$ to 3% . This interpretation is consistent with the petrographic data (see section 3.1).

233 Most of nitrogen is released at low T ($200\text{-}700^\circ\text{C}$) and appears to predominantly reflect
234 terrestrial contamination. Isotopically it is relatively heavy and has a comparatively high (~ 0.1) C/N
235 ratio that also points to terrestrial organic contamination. The extension of the low T peak of nitrogen
236 to 700°C suggests that a part of the nitrogen is associated with the secondary carbonate.

237

238 3.3. NWA 7325, a unique achondrite.

239

240 3.3.1. What is the parent body of NWA 7325?

241 As pointed out by Irving et al. (2013), various major element ratios (e.g., Al/Si and Mg/Si)
242 determined from NWA 7325 are within the range of values measured on Mercury's surface by remote
243 sensing observations (Weider et al., 2012). However, the suggestion that NWA 7325 may represent a
244 sample of Mercury's crust (Irving et al., 2013) has been challenged on the basis of dating evidence.
245 Amelin et al. (2013) obtained a Pb-isotopic age for NWA 7325 of 4562.5 ± 4.4 Ma. This very old age
246 was subsequently confirmed by Dunlap et al. (2014), who obtained an Al-Mg age of 4562.8 ± 0.3 Ma.
247 Both teams pointed out that NWA 7325 crystallized at the same time as angrites and some other
248 achondrites, and seems too old to be a sample of the differentiated crust of a planetary-sized body.
249 Therefore, a mercurian origin appears to be untenable, and instead it seems more likely that NWA
250 7325 originated from one of the planetesimals that formed during the first millions of years after the
251 formation of refractory inclusions.

252

253 Achondrites display a wide range of mineralogical compositions (e.g., Mittlefehldt et al., 1998).
254 Even if these rocks sampled a limited number of differentiated bodies, they formed under a variety of

255 conditions, and illustrate, at least partially, the diversity of primitive materials and conditions present
256 in the early Solar System (i.e., highly reduced conditions for aubrites, a volatile-depleted body and
257 more oxidized conditions for angrites, C-rich body with ureilites...). Despite this large mineralogical
258 variability, achondrites displaying highly magnesian silicates and calcic plagioclases are exceptional.
259 Only a unique mm-sized troctolitic clast found in the polymict ureilite Dar al Gani 319 displays phase
260 compositions similar to NWA 7325 (plagioclase An₈₇₋₈₉, olivine Fo₉₃, Ikeda et al., 2000; Kita et al.,
261 2004; Goodrich et al., 2014). Although the O-isotopic composition of NWA 7325 is in the range of the
262 ureilites (Fig. 4), two important lines of evidence preclude these meteorites originating from the same
263 body:

264 (i) Olivine cores in ureilites display a wide range of compositions which are correlated with the O
265 isotopic composition of the bulk rocks (Clayton and Mayeda, 1996). If NWA 7325 formed from an
266 ureilitic source, the latter would necessarily be among the most Mg-rich ureilites, which display the
267 lowest $\Delta^{17}\text{O}$ values (< -2 ‰), inconsistent with the $\Delta^{17}\text{O}$ value of NWA 7325 (Fig. 6).

268

269 (ii) While ureilites display a restricted range of $\epsilon^{54}\text{Cr}$ values close to -0.9 (e.g., Yamakawa et al.,
270 2010), NWA 7325 has a distinct $\epsilon^{54}\text{Cr}$ value of -0.55 ± 0.08 , precluding this meteorite originating from
271 the ureilite parent body (Sanborn et al., 2013).

272

273 Thus, NWA 7325 is a unique achondrite with distinctive geochemical and isotopic features. It
274 certainly originated from a parent body unsampled by other achondrites. In Figure 7, we compare the
275 Ga/Al, Zn/Al and Na/Al ratios in NWA 7325 (analyses from the interior chip, not the cutting dust
276 samples) with other well-characterized achondrites. Unlike the martian achondrites, the ureilitic
277 (ALM-A) and brachinitic (GRA-06) melts, NWA 7325 displays low Na/Al, Ga/Al and Zn/Al and plots
278 near or in the fields of rocks from the Moon and Vesta, suggesting a volatile-depleted parent body.
279 This inference is strengthened by the very low K, Rb and Cs abundances shown by the NWA 7325
280 chip (Table 3).

281

282 3.3.2. Petrology of NWA 7325

283 Discussing the petrology of a gabbroic rock that is the sole sample we have at present from an
284 unknown parent body is a challenging task. The huge positive Eu anomaly displayed by NWA 7325 is
285 unambiguously related to its abundant plagioclases and points to reduced conditions (e.g., Drake and
286 Weill, 1975), in agreement with the occurrence of traces of metal, Cr-rich sulfides. Indeed, the
287 valences of Cr, Ti, V in olivine and pyroxene determined by XANES spectroscopy suggest
288 crystallization conditions close to the Cr-CrO buffer (i.e. fO_2 close to IW-4, Sutton et al., 2014).

289
290 Gabbroic rocks displaying positive Eu anomalies are widely considered as cumulates. NWA
291 7325 is no exception (e.g., Irving et al., 2013), but we emphasize that this interpretation is not unique.
292 Significant positive Eu anomalies can be generated in non-cumulative basaltic rocks by partial
293 melting, for example during short duration reheating events (Yamaguchi et al., 2009; 2013). Larger
294 degrees of melting of a basaltic or gabbroic lithology can produce gabbroic restites displaying very
295 low incompatible trace element abundances and huge positive anomalies. Previous studies have
296 emphasized the complex thermal history of NWA 7325, and shown that its texture could be explained
297 by remelting (e.g., Bischoff et al., 2013). Thus, the possibility that NWA 7325 could be a restite merits
298 further consideration.

299
300 Partial melting has been previously proposed to explain the very low REE abundances and
301 very large Eu anomalies displayed by some gabbroic pebbles found in mesosiderites (e.g., Rubin and
302 Mittlefehldt, 1992). We analyzed for comparison two such pebbles from Vaca Muerta (Table 2 and
303 Figures 2 and 3). These meteorites are finds from the Atacama Desert. They display some anomalies
304 that are certainly the result of terrestrial weathering, and that do not require further consideration here,
305 i.e. positive Ce anomalies, sometimes high U/Th ratios and high Pb abundances, etc... Interestingly,
306 these two pebbles display at first glance the same level of incompatible trace element concentrations
307 and the same large Sr and Eu anomalies as NWA 7325. However, their REE patterns display marked
308 heavy-REE enrichments ($Gd_n/Lu_n = 0.14-0.43$) which are well explained by the loss of a partial melt
309 (e.g., Yamaguchi et al., 2009). The REE pattern of the NWA 7325 chip does not exhibit such an

310 enrichment ($Gd_n/Lu_n = 2.92$). We conclude that NWA 7325 is probably not restitic, although we note
311 that this inference is model dependent (i.e., composition of the melted lithology).

312

313 If NWA 7325 is a cumulate, what can we infer about the composition of its parental melt
314 based on its petrography and major and trace element abundances? It was certainly “basaltic”, not
315 SiO_2 -saturated (crystallization of olivine), and Ca-rich (diopsidic pyroxene and calcic plagioclase). It
316 was certainly Na-poor (calcic plagioclase) and of course displayed a very low FeO/MgO in order to
317 explain the very high Mg/(Fe+Mg) ratios of the olivines and pyroxenes. Moreover, NWA 7325
318 displays very low abundances of incompatible trace elements. Its parental melt was certainly very poor
319 in these elements. While it is not possible to precisely constrain its trace element abundances, some
320 very simple assumptions allow us to qualitatively evaluate some of its features. Partition coefficients
321 for Yb or Lu in diopside are about 10 times larger than those for plagioclase or olivine (e.g., McKay et
322 al., 1989; Schosnig and Hoffer, 1998). Consequently, in a cumulate like NWA 7325, made essentially
323 of plagioclase, diopsidic pyroxene and olivine, the pyroxene controls the budget of heavy REEs.
324 Assuming that the NWA 7325 chip contained about 33 wt% pyroxene, the Yb or Lu concentrations in
325 this mineral are probably $\approx 0.15 \times CI$ abundances. Partition coefficients of Yb for diopside at low
326 pressure range from 0.1 and 0.6 (Schosnig and Hoffer, 1998, and references therein) suggesting Yb or
327 Lu abundances in the range of 0.25 to $1.5 \times CI$ abundances only in the parental melt. Furthermore, the
328 shape of its REE pattern was probably not chondritic. Again, since clinopyroxene controls the heavy
329 REE abundances in NWA 7325, the Gd-Lu part of the REE pattern is chiefly controlled by its partition
330 coefficients and the $(Gd/Lu)_n$ of the parental melt. Because $(D_{Gd}/D_{Lu})_{cpx}$ is ≈ 1 (e.g., Schosnig and
331 Hoffer, 1998), $(Gd/Lu)_n$ ratios close to 1 are expected for pure cumulates formed from a chondritic
332 melt. This inference remains valid even if the cumulates contain some trapped melt. As a consequence,
333 the high $(Gd/Lu)_n$ ratio ($=2.92$) displayed by the NWA 7325 chip is inconsistent with a parental melt
334 displaying a flat REE pattern. The parental melt to NWA 7325 must therefore have had a fractionated
335 REE pattern with $(Gd/Lu)_n$ ratio > 1 , and probably ≈ 3 . Similar lines of reasoning are possible for Eu.
336 Partition coefficients for Eu in plagioclase are much larger than those in pyroxene or olivine (e.g.,
337 McKay et al., 1989; Schosnig and Hoffer, 1998). Therefore, the budget of Eu in the rock is strongly

338 controlled by plagioclase. Assuming that the NWA 7325 chip contained about 53 wt% plagioclase, the
339 Eu concentration in this phase is $\approx 16 \times$ CI abundance. Partition coefficients for Eu in plagioclase are
340 not only dependent on the composition of the melt but are also strongly sensitive to the oxygen
341 fugacity (e.g., McKay, 1989). For the purpose of calculation, partition coefficients for Eu in calcic
342 plagioclase at low fO_2 for a basaltic melt are assumed to range from 0.7 to 1.1 as suggested by McKay
343 (1989), and in agreement with the recent experimental results obtained by Rapp et al. (2015). The Eu
344 concentration of the parental melt was probably in the range of 14 to 23 \times CI abundances. Even if we
345 take into account the enrichment in middle REEs of the parental melt (i.e., the $(Gd/Yb)_n$ or the
346 $(Gd/Lu)_n$ ratios), its level of concentration of Eu is very high compared to the heavy-REEs. It comes as
347 an unavoidable conclusion that the parental melt of NWA 7325 certainly displayed a very large
348 positive Eu anomaly ($Eu_n/Yb_n > 10$, probably $Eu_n/Gd_n > 3$) that is difficult to estimate accurately.

349 A melt with such a large positive Eu is very unlikely to be the direct product of the early
350 magmatic activity on a planetesimal. On the other hand, gabbros formed in reduced conditions can
351 display low incompatible trace element abundances and large positive Eu, as exemplified by the
352 cumulate eucrites. Total melting of such rocks could produce melts with these features. It is tempting
353 to propose that NWA 7325 is a cumulate derived from the crystallization of such a melt, with the
354 melting of its protolith possibly produced by an energetic impact.

355

356 Recent data for NWA 7325 allow us to further evaluate this hypothesis. Highly Siderophile
357 Elements (HSEs) are sensitive tracers of chondritic contributions in impact melts and impactites. Two
358 samples were analyzed by Archer et al. (2015). Their abundances differ from one another by almost
359 one order of magnitude, and demonstrate that the HSE carriers are heterogeneously distributed in the
360 bulk rock. The sample displaying the highest abundances shows a chondritic distribution of HFES, in
361 agreement with a possible projectile contribution (it contains about 0.9 ng/g Ir, suggesting the addition
362 of ≈ 0.2 wt% of chondritic material). Archer et al. (2015) suggested that this chondritic signature was
363 introduced into the rock after crystallization during late-stage impacts. Because NWA 7325 is
364 unbrecciated, this explanation is unlikely. Alternatively, a chondritic component could have been
365 introduced into the NWA 7325 parental melt during its crystallization. One possibility is that NWA

366 7325 became contaminated through interaction with regolith material. The parental melt could have
367 inefficiently assimilated regolith containing chondritic debris. However, as pointed out by Archer et al.
368 (2015), an assimilation process that only partially affected the rock, is difficult to envisage. Instead, a
369 heterogeneously distributed chondritic signature in NWA 7325 is best explained if this meteorite was
370 derived from the crystallization of an impact melt.

371 Moreover, the systematics of ^{26}Al - ^{26}Mg further strengthens the hypothesis that NWA 7325
372 formed by impact-melting of gabbroic material. The Al-Mg internal isochron obtained previously by
373 Dunlap et al. (2014) for NWA 7325 has a well-resolved positive intercept ($\delta^{26}\text{Mg}_0^*$) of 0.095 ± 0.011
374 ‰, and lies well above the bulk chondritic value (Al/Mg \approx 0.1 and $\delta^{26}\text{Mg}^* \approx$ 0 ‰). As noted by
375 Dunlap et al. (2014), this high $\delta^{26}\text{Mg}_0^*$ could imply a non-chondritic initial composition for the
376 parental body. Alternatively, the source material for this achondrite may have evolved with a highly
377 superchondritic Al/Mg ratio early in the history of the solar system prior to the heating event that
378 formed the melt that was parental to NWA 7325. Gabbros and plagioclase-rich cumulates are Al-rich
379 compared to chondrites, and exhibit highly superchondritic Al/Mg ratios. The impact-melting
380 hypothesis of this kind of rock offers a straightforward explanation for the distinctly high $\delta^{26}\text{Mg}_0^*$ of
381 NWA 7325 (Fig. 8). Moreover, assuming that the parental melt of NWA 7325 formed by impact
382 melting of a gabbroic target 4.5628 Ga ago, we can place some constraints on the formation age of its
383 protolith. Unfortunately, the $^{27}\text{Al}/^{24}\text{Mg}$ ratio of the parental melt of NWA 7325 is not known. Because
384 NWA 7325 is a plagioclase rich cumulate, its parental melt displayed probably a lower Al abundance
385 than the whole rock, but it is not possible to assess neither its Mg concentration nor its Al/Mg ratio. In
386 the case of eucrites, the Al/Mg ratios of cumulate and basaltic eucrites are similar. Although these
387 rocks are probably not perfect analogs of NWA 7325, we can reasonably propose that the situation
388 was comparable for NWA 7325 and its parental melt. For the purpose of calculation, we used the
389 whole rock $^{27}\text{Al}/^{24}\text{Mg}$ ratio (= 1.56) and we obtained an intercept with the solar system growth curve at
390 about 4566 Ma. A lower Al/Mg ratio would point to an older model age, and conversely younger
391 model ages are obtained with higher Al/Mg ratios, but variations of 25 % around the Al/Mg ratio of
392 the whole rock do not alter this estimation (Fig. 9). Although only indicative, our calculations show

393 that remelting of a very old gabbroic lithology can perfectly explain the high $\delta^{26}\text{Mg}^*_0$ of NWA 7325.
394 Thus, NWA 7325 provides evidence of one of the earliest crusts on a differentiated body so far
395 studied. We note that the NWA 7325 protolith could be practically contemporaneous to Asuka
396 881394, which formed 4566.5 ± 0.2 Ma ago on a distinct parent body (Wadhwa et al., 2009).

397

398 4. Conclusions

399 Two important conclusions emerge from this study. The first one is methodological. While it
400 is often very difficult to obtain representative samples of rare meteorites, the use of cutting dust should
401 be avoided, at least for the trace element analyses. Secondly, our data confirm that NWA 7325 is a
402 new type of achondrite that originated from a parent body not previously sampled by the other
403 meteorites. Despite their similar oxygen isotope compositions, a number of lines of evidence preclude
404 a relationship between NWA 7325 and the ureilites. NWA 7325 is a gabbroic rock that displays
405 distinct phase compositions, notably highly magnesian pyroxenes and olivine. Its chemical
406 composition suggests that it formed from an unusual melt characterized by very low incompatible
407 trace element abundances and a very large positive Eu anomaly. We propose that this melt formed by
408 the remelting of an ancient gabbroic lithology, possibly upon impact, in agreement with the HSE
409 abundances, and the systematics of ^{26}Al - ^{26}Mg . Based on recent dating, the crustal material that was
410 parental to NWA 7325 must have been older than 4562.8 Ma. Thus, NWA 7325 provides evidence of
411 one of the earliest crusts on a differentiated body so far studied and indicates how such materials were
412 rapidly recycled.

413 *Acknowledgements*

414 The Vaca Muerta samples were given a long time ago to one of us (JAB) by our late colleague
415 Gérard Poupeau. We thank Christian Koeberl for the editorial handling, Tim Fagan and an anonymous
416 reviewer for constructive comments, Marc Chaussidon for discussions, and Pascale Barrat for her
417 help. Special thanks to Stefan Ralew for the pictures of the hand specimens and the cutting dust
418 sample, and to John Kashuba for the thin section picture. We gratefully acknowledge the Programme
419 National de Planétologie (CNRS-INSU) for financial support. Stable isotope analysis at the Open
420 University is funded by a consolidated grant from STFC. This research has made use of NASA's
421 Astrophysics Data System Abstract Service.

422

423

References

- 424 Amelin Y., Koefoed P., Iizuka T., Irving A.J. (2013) U-Pb age of ungrouped achondrite NWA 7325. *76th Annual*
425 *Meteoritical Society Meeting*, abstract # 5165.
- 426 Archer G.J., Walker R.J., and Irving A.J. (2015) Highly siderophile element and 187Re-187Os isotopic
427 systematics of ungrouped achondrite Northwest Africa 7325. *46th Lunar Planet. Sci. Conf.*, abstract # 1987.
- 428 Barrat J.A., Gillet Ph., Lesourd M., Blichert-Toft J. and Poupeau G.R. (1999) The Tatahouine diogenite:
429 mineralogical and chemical effects of 63 years of terrestrial residence. *Meteoritics Planet. Sci.* **34**, 91-97.
- 430 Barrat J.A., Jambon A., Bohn M., Blichert-Toft J., Sautter V., Göpel C., Gillet Ph., Boudouma O., and Keller F.
431 (2003) Petrology and geochemistry of the unbrecciated achondrite North West Africa 1240 (NWA 1240):
432 an HED parent body impact melt. *Geochim. Cosmochim. Acta* **67**, 3959-3970.
- 433 Barrat J.A., Yamaguchi A., Zanda B., Bollinger C., Bohn M. (2010) Relative chronology of crust formation on
434 asteroid 4-Vesta: Insights from the geochemistry of diogenites. *Geochim. Cosmochim. Acta.* **74**, 6218-6231.
- 435 Barrat J.A., Zanda B., Moynier F., Bollinger C., Liorzou C., and Bayon G. (2012) Geochemistry of CI
436 chondrites: Major and trace elements, and Cu and Zn isotopes. *Geochim. Cosmochim. Acta* **83**, 79-92.
- 437 Barrat J.A., Zanda B., Jambon A., Bollinger C. (2014) The lithophile trace elements in enstatite chondrites.
438 *Geochim. Cosmochim. Acta.* **128**, 71-94.
439
- 440 Bischoff A., Ward D., Weber I., Morlok A., Hiesinger H., Helbert J. (2013) NWA 7325 – not a typical olivine
441 gabbro, but a rock experienced fast cooling after a second (partial) melting. *European Planet. Sci. Congress*
442 **8**, EPSC2013-427 (abstract).
443
- 444 Bischoff A., Horstmann M., Barrat J.A., Chaussidon M., Pack A., Herwartz D., Ward D., Vollmer C., Decker S.
445 (2014) trachyandesitic volcanism in the early Solar System. *PNAS* **111**, 35, 12689-12692.
446
- 447 Clayton R.N., Mayeda T.K. (1996) Oxygen isotope studies of achondrites. *Geochim. Cosmochim. Acta* **60**, 1999-
448 2017.
449
- 450 Clayton R.N., Mayeda T.K. (1999) Oxygen isotope studies of carbonaceous chondrites. *Geochim. Cosmochim.*
451 *Acta* **63**, 2089-2104.
452
- 453 Crozaz G., Floss C., and Wadhwa M. (2003). Chemical alteration and REE mobilization in meteorites from hot
454 and cold deserts. *Geochim. Cosmochim. Acta* **67**, 4727-4741.
455
- 456 Day J.M.D. *et al.* (2012) Origin of felsic achondrites Graves Nunataks 06128 and 06129, and ultramafic
457 brachinites and brachinite-like achondrites by partial melting of volatile-rich primitive parent bodies.
458 *Geochim. Cosmochim. Acta* **81**, 94–128.
459
- 460 Downes, H., Mittlefehldt, D.W., Kita, N.T., Valley, J.W. (2008) Evidence from polymict ureilite meteorites for a
461 disrupted and re-accreted single ureilite parent asteroid gardened by several distinct impactors. *Geochim*
462 *Cosmochim Acta* **72**, 4825–4844.
463
- 464 Downes, H., Abernethy, F. A. J., Smith, C. L., Ross, A. J., Verchovsky, A. B., Grady, M. M., Jenniskens, P., and
465 Shaddad, M. H. (2015) Isotopic composition of carbon and nitrogen in ureilitic fragments of the Almahata
466 Sitta meteorite, *Meteoritics Planet. Sci.* **50**, 255-272.
467
- 468 Drake M. J. and Weill D. F. (1975) Partition of Sr, Ba, Eu²⁺, Eu³⁺, and other REE between plagioclase feldspar
469 and magmatic liquid: An experimental study. *Geochim. Cosmochim. Acta* **39**, 689–712.
470
- 471 Dunlap D.R., Wadhwa M., Romaneillo S.R. (2014) ²⁶Al-²⁶Mg systematics in the unusual ungrouped achondrite
472 NWA 7325 and the eucrite Juvinas. *45th Lunar Planet. Sci. Conf.*, abstract # 2186.

473
474 El Goresy A., Nakamura T., Miyahara M., Ohtani E., Gillet P., Jogo K., Yamanobe M., Ishida H. (2014) The
475 unique differentiated meteorite NWA 7325: highly reduced, stark affinities to E-chondrites and unknown
476 parental planet. *77th annual Meteoritical Society Meeting*, abstract # 5028.
477
478 Goodrich, C. A., Wlotzka, F., Ross, D. K. and Bartoschewitz, R. (2006) NWA 1500: plagioclase-bearing
479 monomict ureilite or ungrouped achondrite? *Meteoritics Planet. Sci.* **41**, 925–952.
480
481 Goodrich C.A., Harlow G.E., Van Orman J.A., Sutton S.R., Jercinovic M.J., Mikouchi T. (2014) Petrology of
482 chromite in ureilites: Deconvolution of primary oxidation states and secondary reduction processes.
483 *Geochim. Cosmochim. Acta* **135**, 126-169.

484 Goodrich C.A., Kita N.T., Nakashima D. (2014) Petrology of the NWA 7325 ungrouped achondrite – Meteorite
485 from Mercury, the Ureilite Parent Body, or a previously unsampled asteroid? *45th Lunar Planet. Sci. Conf.*,
486 abstract # 1246.
487
488 Greenwood R.C., Franchi I.A., Jambon A., Barrat J.A., Burbine T.H. (2006) Oxygen isotope variation in stony-
489 iron meteorites. *Science* **313**, 1763-1765.

490 Greenwood R.C., Barrat J.A., Yamaguchi A., Franchi I.A., Scott E.R.D., Bottke W.F., Gibson J.M. (2014) The
491 oxygen isotope composition of diogenites: Evidence for early global melting on a single, compositionally
492 diverse, HED parent body. *Earth Planet. Sci. Lett.* **390**, 165-174.
493
494 Greenwood R.C., Franchi I.A., Gibson J.M., Benedix G.K. (2012) Oxygen isotope variation in primitive
495 achondrites: The influence of primordial, asteroidal and terrestrial processes. *Geochim. Cosmochim. Acta*
496 **94**, 146–163.
497
498 Irving A.J., Kuehner S.M., Bunch T.E., Ziegler K., Chen G., Herd C.D.K., Conrey R.M., Ralew S. (2013)
499 Ungrouped mafic achondrite Northwest Africa 7325: a reduced, iron poor cumulate olivine gabbro from a
500 differentiated planetary body. *44th Lunar Planet. Sci. Conf.*, abstract #2164.
501
502 Jabeen I., Ali A., Banerjee N.R., Osinski G.R., Ralew S., DeBoer S. (2014) Oxygen isotope compositions of
503 mineral separates from NWA 7325 suggest a planetary (Mercury?) origin. *45th Lunar Planet. Sci. Conf.*,
504 abstract # 2215.
505
506 Keil K. (2010) Enstatite achondrite meteorites (aubrites) and the histories of their asteroidal parent bodies.
507 *Chemie der Erde-Geochemistry* **70**, 295–317.
508
509 Keil K. (2012) Angrites, a small but diverse suite of ancient, silica-undersaturated volcanic-plutonic mafic
510 meteorites, and the history of their parent asteroid. *Chemie der Erde* **72**, 191-218.
511
512 Keil, K. (2014) Brachinite meteorites: Partial melt residues from an FeO-rich asteroid. *Chemie der Erde* **74**, 311-
513 329.
514
515 Kita N.T., Sanborn M.E., Yin Q.Z., Goodrich C.A. (2014) The NWA 7325 ungrouped achondrite – Possible link
516 to ureilite? Oxygen and chromium isotopes and trace element abundances. *45th Lunar Planet. Sci. Conf.*,
517 abstract # 1455.
518
519 Love S.G., Keil K. (1995) Recognizing mercurian meteorites. *Meteoritics* **30**, 269-278.
520
521 McKay G. A. (1989) Partitioning of rare earth elements between major silicate minerals and basaltic melts. *Rev.*
522 *Mineral. Geochem.* **21**, 45–77.
523
524 Miller M.F. (2002) Isotopic fractionation and the quantification of ¹⁷O anomalies in the oxygen three isotopes
525 system: an appraisal and geochemical significance. *Geochim. Cosmochim. Acta* **66**, 1881-1889.
526
527 Miller M.F., Franchi I.A., Sexton A.S., Pillinger C.T. (1999) High precision ¹⁷O isotope measurements of
528 oxygen from silicates and other oxides: Method and applications. *Rapid Commun. Mass Spectrom.* **13**, 1211-
529 1217.
530

531 Mittlefehldt, D.W., McCoy, T.J., Goodrich, C.A., Kracher, A. (1998) Non-chondritic meteorites from asteroidal
532 bodies. In: Papike, J.J. (Ed.), Planetary Materials. Mineralogical Society of America, Washington, DC, 195
533 pp.
534

535 Perkins D., Vielzeuf D. (1992) Experimental investigation of Fe-Mg distribution between olivine and
536 clinopyroxene: Implications for mixing properties of Fe-Mg in clinopyroxene and garnet-clinopyroxene
537 thermometry. *American Mineralogist* **77**, 774-783.
538

539 Pouchou, J.L., Pichoir, F. (1985) 'PAP' procedure for improved quantitative microanalysis. *Microbeam Anal.*
540 **54**, 104-106.
541

542 Rapp J.F., Lapen T.J., Draper D.S. (2015) REE partitioning in lunar minerals. 46th Lunar Planet. Sci. Conf.,
543 abstract # 2878.
544

545 Rubin A.E., Mittlefehldt D.W. (2012) Classification of mafic clasts from mesosiderites: implications for
546 endogenous igneous processes. *Geochimica Cosmochimica Acta* **56**, 827-840.
547

548 Sanborn M.E., Yamakawa A., Yin Q.Z., Irving A.J., Amelin Y. (2013) Chromium isotopic studies of ungrouped
549 achondrites NWA 7325, NWA 2976, and NWA 6704. 76th Annual Meteoritical Society Meeting, abstract #
550 5220.
551

552 Schosnig M., Hoffer E. (1998) Compositional dependence of REE partitioning between diopside and melt at 1
553 atmosphere. *Contrib. Mineral. Petrol.* **133**, 205-216.
554

555 Singletary, S. J. and Grove, T. L. (2003) Early petrologic processes on the ureilite parent body. *Meteorit. Planet.*
556 *Sci.* **38**, 95-108.
557

558 Stelzner T., Heide K., Bischoff A., Weber A., Weber D., Scherer P., Schukz L., Happel M., Schrön W., Neupert
559 U., Michel R., Clayton R. N., Mayeda T. K., Bonani G., Haidas I., Ivy-Ochs S., and Suter M. 1999. In
560 interdisciplinary study of weathering effects in ordinary chondrites from the Acfer region Algeria.
561 *Meteoritics Planet. Sci.* **34**, 787-794.
562

563 Sutton S.R., Wirick S., Goodrich C.A. (2014) Ungrouped achondrite NWA 7325: titanium, vanadium and
564 chromium XANES of mafic silicates record highly-reduced origin. 45th Lunar Planet. Sci. Conf., abstract #
565 1275.
566

567 Verchovsky, A.B., Fisenko, A.V., Semjonova, L.F., Wright, I.P., Lee, M.R., Pillinger, C.T. (1998) C, N, and
568 noble gas isotopes in grain size separates of presolar diamonds from Efremovka. *Science* **281**, 1165-1168.

569 Verchovsky, A.B., Sephton, M.A., Wright, I.P., Pillinger, C.T. (2002) Separation of planetary noble gas carrier
570 from bulk carbon in enstatite chondrites during stepped combustion. *Earth Planetary Science Letters* **199**,
571 243-255.

572 Wadhwa M., Hamelin Y., Bogdanovski O., Shukolyukov A., Lugmair G.W., Janney P. (2009) Ancient relative
573 and absolute ages for a basaltic meteorite: Implications for timescale of planetesimal accretion and
574 differentiation. *Geochim. Cosmochim. Acta* **73**, 5189-5201.

575 Warren P.H., Rubin A.E., Isa J., Brittenham S., Ahn I., Choi B.G. (2013) Northwest Africa 6693: a new type of
576 FeO-rich, low- $\Delta^{17}\text{O}$, poikilitic cumulate achondrite. *Geochim. Cosmochim. Acta* **107**, 135-154.
577

578 Weber I., Morlok A., Bischoff A., Hiesinger H., Helbert J. (2014) Mineralogical and spectroscopic studies on
579 NWA 7325 as an analogue sample for rocks from Mercury. 45th Lunar Planet. Sci. Conf., abstract # 1323.
580

581 Weider Z.S., Nittler L.R., Starr R.D., McCoy T.J., Stockstill-Cahill K.R., Byrne P.K., Denevi B.W., Head J.W.,
582 Salomon S.C. (2012) Chemical heterogeneity on Mercury's surface revealed by the MESSENGER X-Ray
583 Spectrometer. *J. Geophys. Res.* **117**, E00L05, doi: 10.1029/2012JE004153.
584

585 Yamaguchi A., Clayton R. N., Mayeda T. K., Ebihara M., Oura Y., Miura Y. N., Haramura H., Misawa K.,
586 Kojima H., and Nagao K. (2002) A new source of basaltic meteorites inferred from Northwest Africa 011.
587 *Science* **296**, 334-336.

588
589 Yamaguchi A., Barrat J.A., Greenwood R.C., Shirai N., Okamoto C., Setoyanagi T., Ebihara M., Franchi I.A.,
590 Bohn M. (2009) Crustal partial melting on Vesta : evidence from highly metamorphosed eucrites. *Geochim.*
591 *Cosmochim. Acta* **73**, 7262-7182.
592
593 Yamaguchi A., Mikouchi T., Ito M., Shirai N., Barrat J.A., Messenger S., Ebihara M. (2013) Experimental
594 evidence of fast transport of trace elements in planetary crusts by high temperature metamorphism. *Earth*
595 *Planet. Sci. Lett.* **368**, 101-109.
596
597 Yamakawa A., Yamashita K., Makishima A., Nakamura E. (2010) Chromium isotope systematics of
598 achondrites: Chronology and isotopic heterogeneity of the inner solar system bodies. *Astrophys J.* **720**, 150–
599 154.

600
601
602
603
604

605 Table 1. Average compositions of main phases in NWA 7325 (in wt%).

	n	SiO ₂	TiO ₂	Al ₂ O ₃	Cr ₂ O ₃	FeO	MnO	MgO	CaO	Na ₂ O	K ₂ O	Total	endmembers
plagio.	71	45.25	< 0.03	34.14	< 0.03	0.07	< 0.03	0.29	18.11	1.18	< 0.03	99.07	An _{89.4} Ab _{10.5}
pyrox.	58	52.68	0.04	2.93	1.03	0.73	0.05	18.88	22.54	0.16	< 0.03	99.04	En _{53.2} Wo _{45.6} Fs _{1.2}
olivine	51	42.25	< 0.03	0.04	0.37	2.81	0.07	54.38	0.35	< 0.03	< 0.03	100.25	Fo _{97.2}
		Si	Ti	Al	Cr	Fe	Mn	Mg	Ca	Na	S	Total	
sulfide	13	0.04	< 0.03	< 0.03	3.57	59.62	< 0.03	0.01	0.15	< 0.03	37.64	101.19	

606

607

608

609 Table 2. Major element compositions of NWA 7325 and two low-Ti Vaca Muerta pebbles (in wt%, *: SiO₂ calculated by difference). Data given by Irving et al. (2013) obtained at University of
610 Alberta, are shown for comparison.
611

612

Lab.	NWA 7325			Vaca Muerta	
	cutting dust		chip	VM3	VM4
	U. Alberta	Brest	Brest	Brest	Brest
SiO ₂	47.09	48.04	(46.4*)	(50.0*)	(46.0*)
TiO ₂	0.01	0.05	0.03	0.04	0.06
Al ₂ O ₃	18.6	18.91	17.83	9.65	13.14
Cr ₂ O ₃	0.40	0.44	0.54	0.36	0.35
FeO	1.57	1.87	0.57	19.72	19.74
MnO	0.03	0.04	0.03	0.60	0.58
MgO	12.13	12.18	13.84	10.84	9.69
CaO	17.94	18.37	20.15	8.30	10.05
Na ₂ O	0.60	0.65	0.63	0.17	0.27
K ₂ O	0.01	0.03	<0.01	0.03	0.02
P ₂ O ₅	0.02	0.03	0.04	0.30	0.12
total	98.40	100.61	100.00*	100.00*	100.00*

613

614

615 Table 3. Trace element abundances in NWA 7325 and in two low-Ti Vaca Muerta pebbles (in $\mu\text{g/g}$).

Lab.	NWA 7325			Vaca Muerta	
	cutting	dust	chip	VM3	VM4
	U. Alberta	Brest	Brest	Brest	Brest
Li	0.53	0.93	0.32	3.86	4.22
Be		0.028	0.002	0.010	0.021
P ₂ O ₅ wt%	0.02	0.043	0.024		
K	83	281	23		
Sc		19.64	24.18	29.38	25.41
Ti		239	106	215	361
V		190	249	83.8	85.3
Mn	230	260	254	4246	4097
Co		21.7	23.5	53.1	38.0
Ni	78	164	57	1278	716
Cu		264	6.76	13.6	14.2
Zn		330	5.23	1.97	1.01
Ga		8.32	8.65	1.36	1.58
Rb	0.37	0.86	0.055	0.14	0.18
Sr	198	195	189	37.0	54.9
Y		0.566	0.152	0.064	0.210
Zr	1.3	1.68	0.080	0.98	0.18
Nb	2.5	0.208	0.026	0.12	0.12
Cs		0.043	0.004	0.010	0.009
Ba	61	67.92	14.92	2.48	1.59
La	0.15	0.421	0.0188	0.0585	0.101
Ce	0.34	0.927	0.0612	0.179	0.279
Pr		0.109	0.00755	0.0201	0.0328
Nd	0.16	0.430	0.0413	0.0801	0.127
Sm	0.05	0.0944	0.0175	0.0165	0.0185
Eu	0.58	0.532	0.499	0.176	0.286
Gd	0.05	0.107	0.0308	0.0124	0.0145
Tb		0.0165	0.00484	0.00192	0.00286
Dy		0.0978	0.0302	0.0117	0.0243
Ho		0.0191	0.00573	0.00272	0.00764
Er		0.0521	0.0133	0.00855	0.0315
Yb		0.0452	0.00985	0.0174	0.0658
Lu		0.00635	0.00126	0.00348	0.0125
Hf	0.44	0.049	0.00340	0.0165	0.0035
Ta		0.0170	0.0009	0.011	0.009
W		0.112	<0.001	0.020	<0.001
Pb		3.91	0.027	2.64	0.19
Th	0.27	0.112	0.00901	0.00661	0.0107
U		0.0409	0.00987	0.00591	0.00295

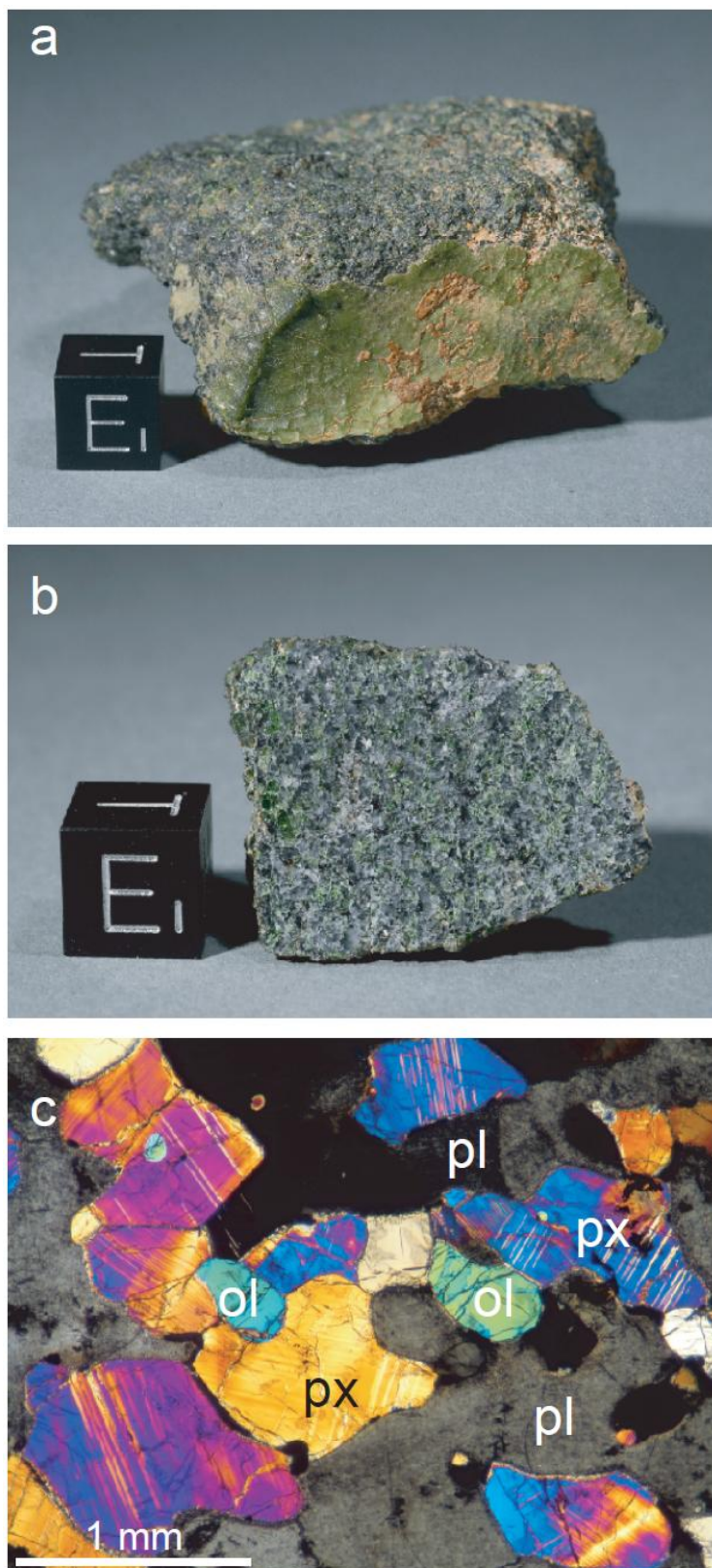
617 Table 4. Nitrogen and Carbon isotope results. The sample weight was 6.143 mg.
 618
 619

T (°C)	C (ng)	$\delta^{13}\text{C}$ (‰)	\pm	N (ng)	$\delta^{15}\text{N}$ (‰)	\pm
200	151	-28.8	0.1	1.82	-4.7	1.4
300	1081	-28.7	0.2	117.7	10.6	0.2
400	533	-27.5	0.2	28.31	4.8	0.2
500	479	-22.2	0.2	23.63	5.5	0.3
600	2241	1.2	0.2	15.53	2.6	0.3
700	2542	3.0	0.2	13.84	3.0	0.4
800	71	-12.6	0.1	3.35	1.1	0.9
900	18	-14.4	0.2	2.17	11.9	1.3
1000	43	-13.1	0.5	0.86	16.5	2.1
1100	8	-16.9	0.2	0.52	-3.1	3.5
1200	15	-22.7	0.2	0.53	11.0	4.1
1300	9	-23.9	0.1	0.42	11.3	5.2
1400	39	-24.9	0.2	0.89	42.5	2.4
	7237	-7.4		210.6	8.0	

620
 621
 622

623

624

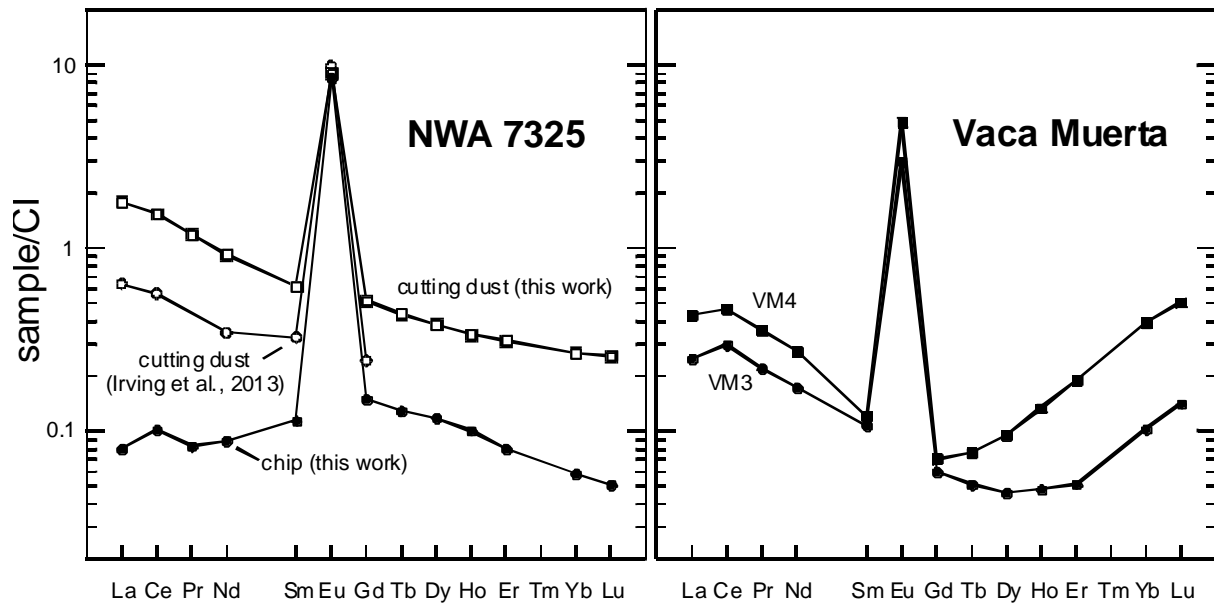


625

626 Figure 1. a: one of the largest NWA 7325 stones; notice the distinctive green fusion crust and the soil
627 materials adhering to the stone; the size of the cube is 1 cm; b: slice of NWA 7325 showing its

628 unbrecciated structure; c: crossed polarized light image of a thin section showing the gabbroic texture.
629 (Pictures a and b, courtesy of Stefan Ralew, picture c, courtesy of John Kashuba).

630

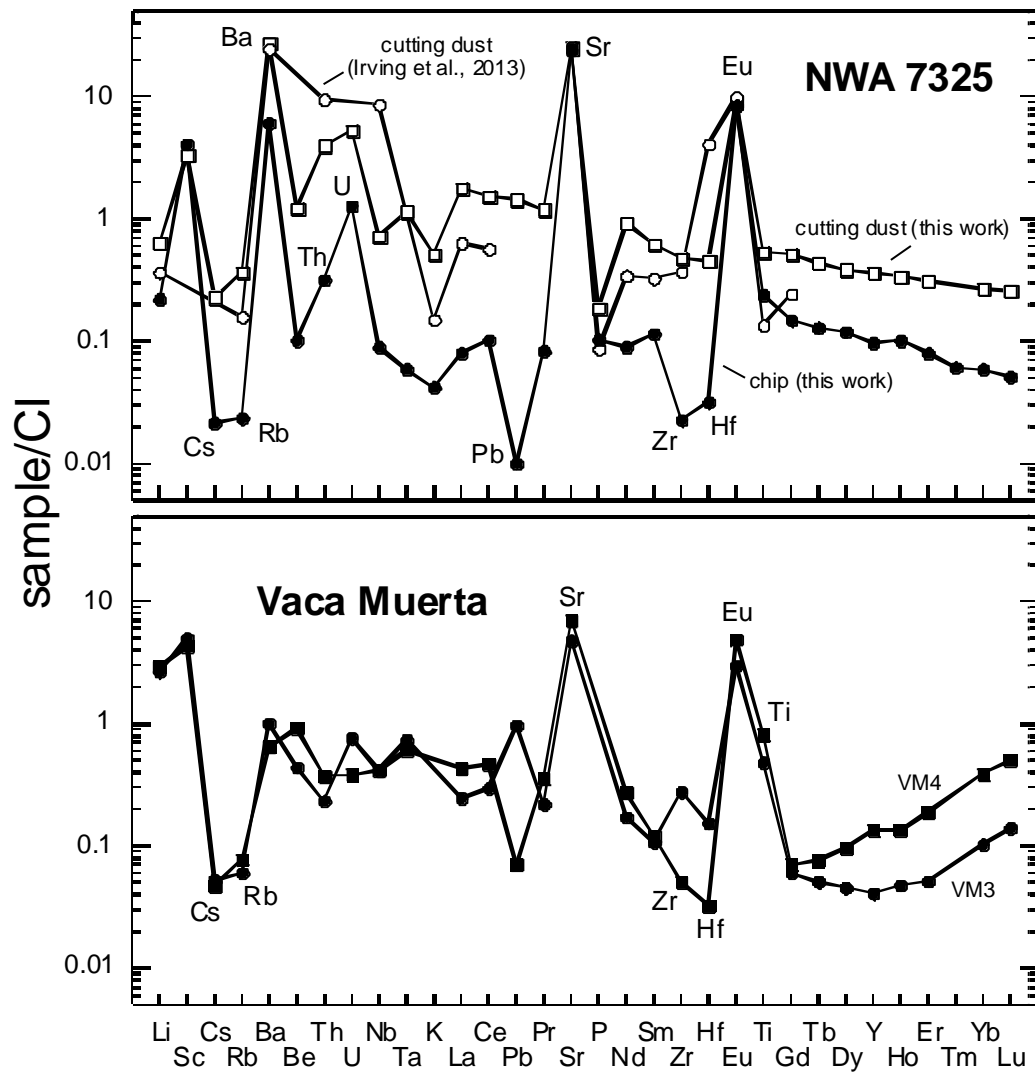


633 Figure 2. REE patterns of NWA 7325 and two low-Ti gabbros from the Vaca Muerta mesosiderite.
634 The reference CI chondrite is from Barrat et al. (2012).

635

636

637



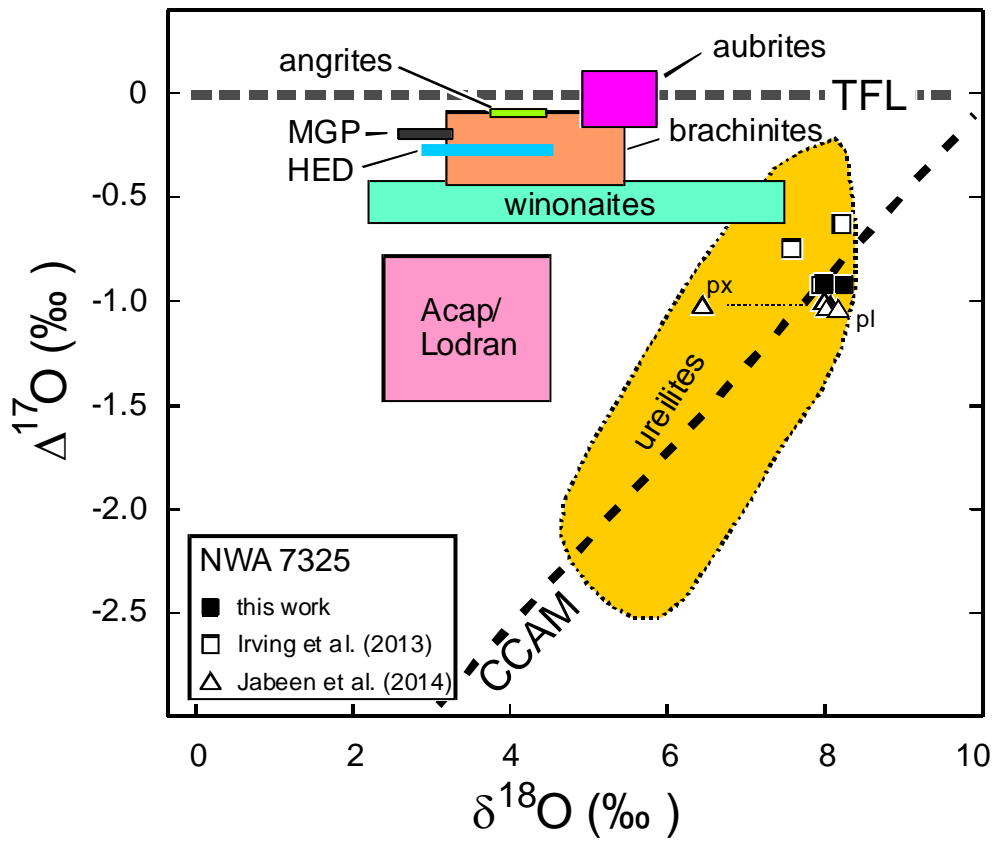
638

639 Figure 3. CI normalized multi-element patterns for NWA 7325 and two low-Ti gabbros from the Vaca
640 Muerta mesosiderite. The reference CI chondrite is from Barrat et al. (2012).

641

642

643



644

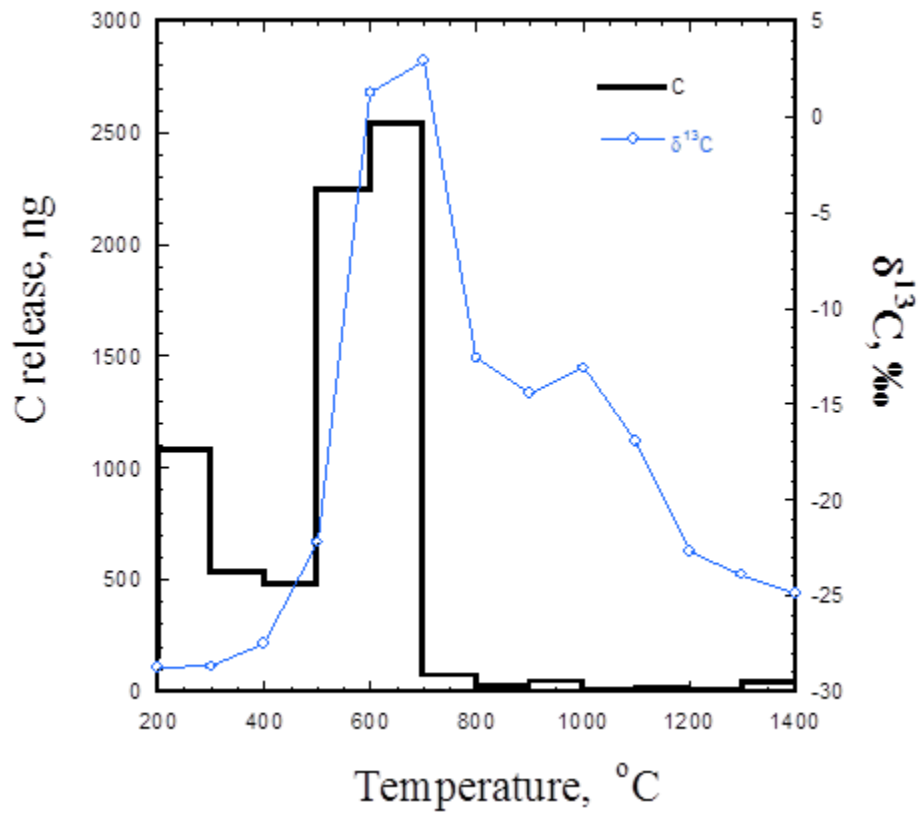
645 Figure 4. Oxygen isotope composition of NWA 7325 (Irving et al., 2013; Jabeen et al., 2014 and this
 646 work) compared with ureilites (Clayton and Mayeda, 1996) and other achondrites (Greenwood et al.
 647 2012, 2014 and references therein). MGP, main-group pallasites; HEDs, howardites, eucrites,
 648 diogenites; TFL, terrestrial fractionation line; CCAM, the carbonaceous chondrite anhydrous mineral
 649 line (Clayton and Mayeda, 1999); Px, pyroxene; Pl, plagioclase.

650

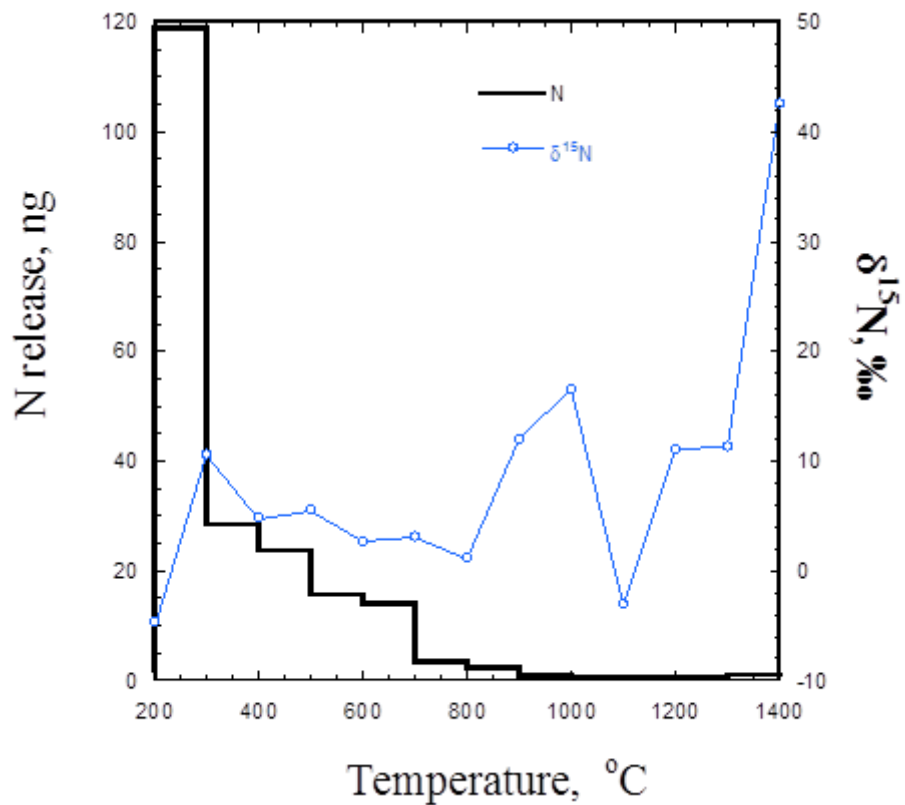
651

652

653

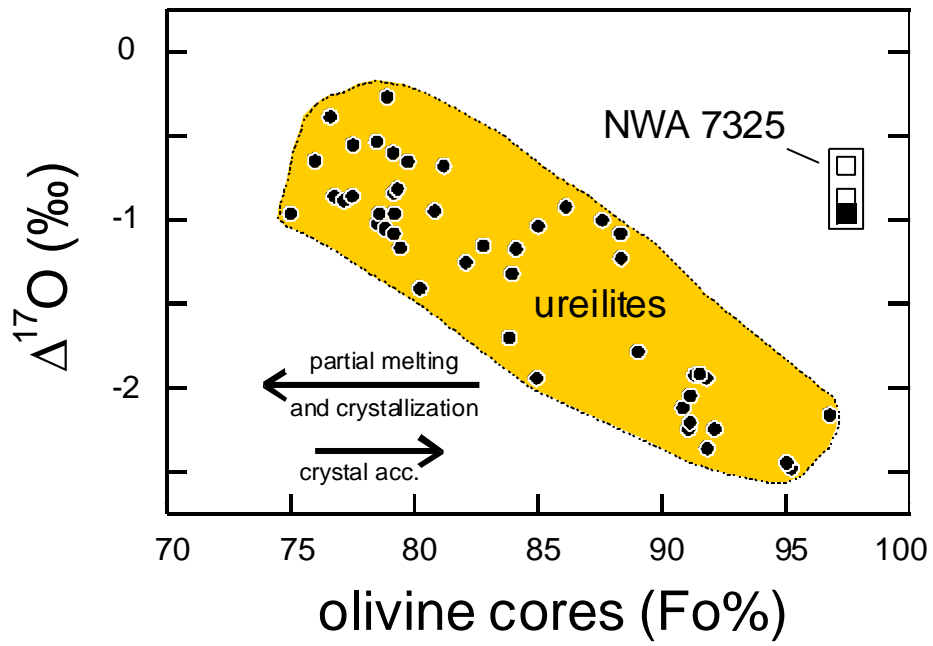


654



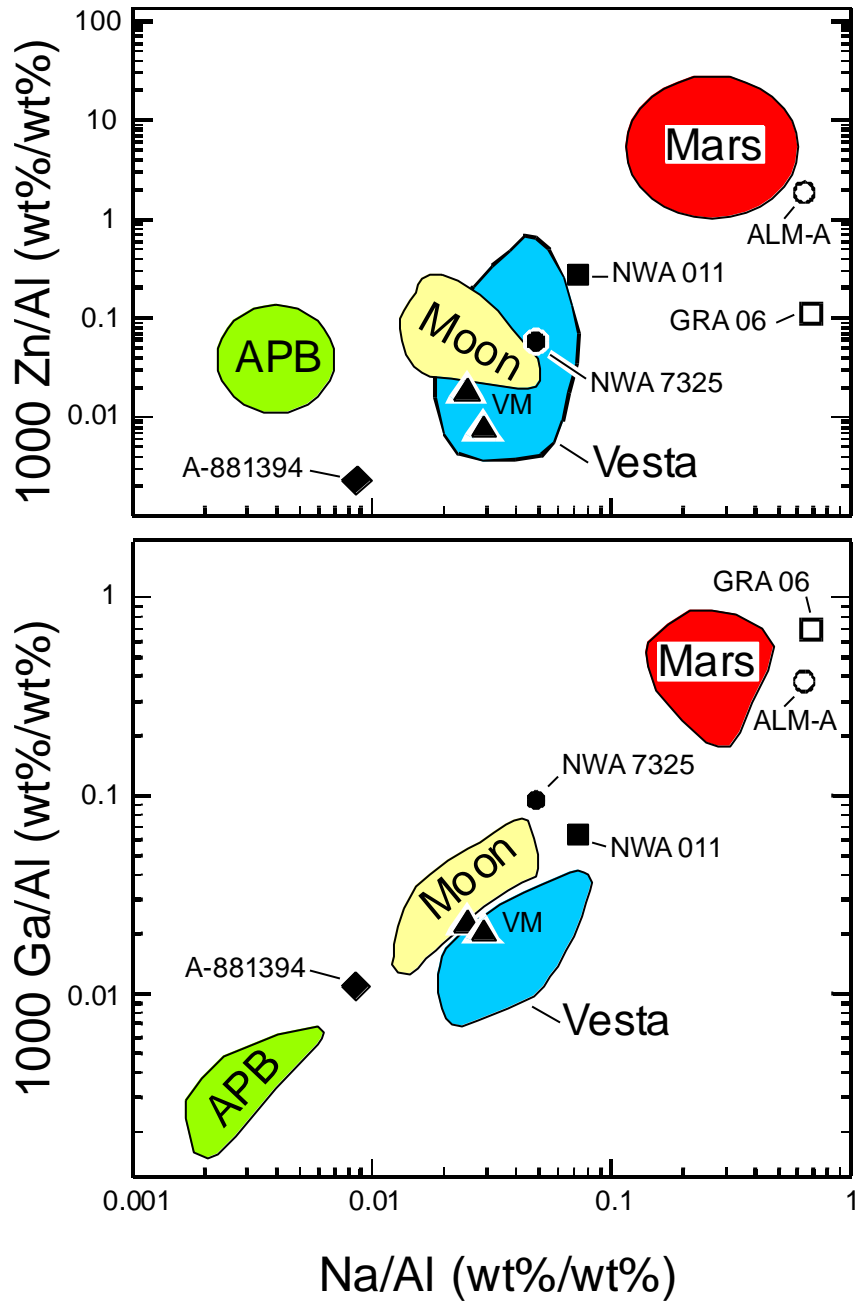
655

656 Figure 5. a: Carbon stepwise combustion results for NWA 7325; b: Nitrogen stepwise combustion results
 657 for NWA 7325.



658

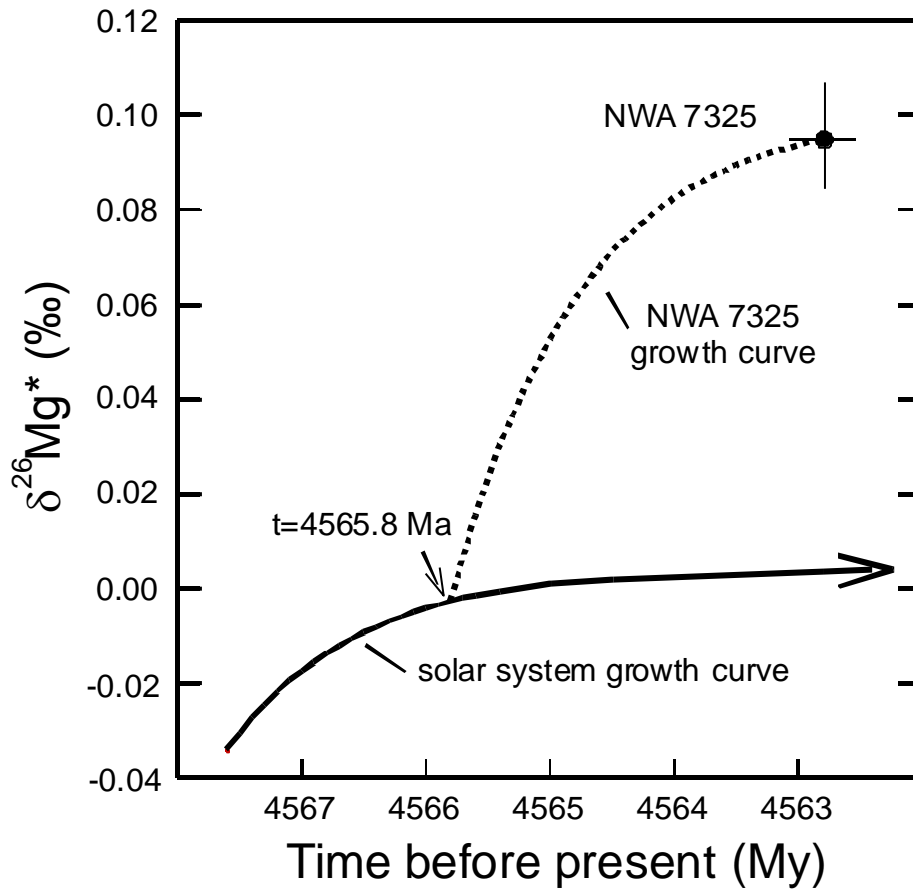
659 Figure 6. Plot of $\Delta^{17}\text{O}$ in the bulk rocks vs. olivine core compositions for ureilites (data from Clayton and
 660 Mayeda (1996), Downes et al. (2008), Singletary and Grove (2003), Goodrich et al. (2006, 2014) and references
 661 therein) and NWA 7425 (Irving et al., 2013 and this work, same symbols as Fig. 3).



662

663 Figure 7. Ga/Al, and Zn/Al vs. Na/Al plots comparing NWA 7325 (chip) and the two Vaca Muerta
 664 Pebbles (VM) with main types of achondrites (fields and data from Warren et al. (2013), Yamaguchi
 665 et al. (2002), Day et al. (2012) and Bischoff et al. (2014)). APB, angrite parent body.
 666

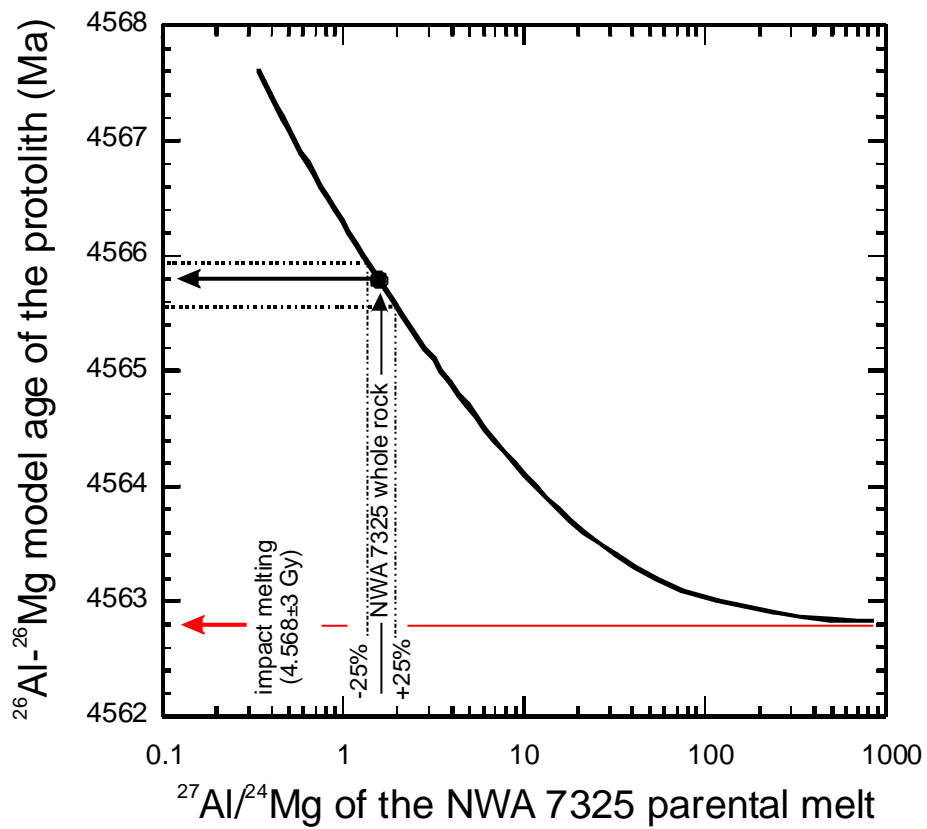
667



668

669 Figure 8. The Mg isotopic composition of NWA 7325 (Dunlap et al., 2014) compared to the
 670 theoretical evolution of the Mg isotopic composition of the solar system (calculated for a chondritic
 671 $^{27}\text{Al}/^{24}\text{Mg}$ ratio of 0.101, a $(^{26}\text{Al}/^{27}\text{Al})_0$ of 5.23×10^{-5} , and a $\delta^{26}\text{Mg}^*_0$ of -0.034 ‰ (Jacobsen et al.,
 672 2008)).

673



675

676

677 Figure 9. Model age of the protolith of NWA 7325 vs. $^{27}\text{Al}/^{24}\text{Mg}$ of its parental melt. Assuming that
 678 the parental melt and the whole rock have the same Al/Mg ratios ($^{27}\text{Al}/^{24}\text{Mg} = 1.56$), an intercept with
 679 the solar system growth curve at about 4566 Ma is obtained.

680

681

682